# Estimation of Constraint Parameters in Optimal Power Flow Data Sets

Daniel K. Molzahn, Zev B. Friedman, Bernard C. Lesieutre, Christopher L. DeMarco, and Michael C. Ferris

***Abstract*—Large-scale electric power system analysis depends upon representation of vast numbers of components whose individual models must be populated with parameters. The challenge of populating such component models is particularly apparent in optimal power flow applications, in which incorrect parameters and/or constraint limits can yield overall system representations with either unrealistically large feasible regions or an empty feasible set. Unfortunately, many data sets, particularly those of publicly available test cases, were originally developed to illustrate simpler "power flow only" applications, and may contain unrealistic values or wholly omit important constraint limits. This paper describes engineering-based approaches to obtain credible estimates for parameters and limits associated with line-flow constraints and generator capability curves, as may be employed in a number of steady state analyses such as the optimal power flow. These can substitute for missing or unrealistic data in test systems for which more fully detailed, "real-world" component specifications and limits are not available, and thereby make such test systems more valuable as research tools.**

***Index Terms*—Power system modeling, Optimal power flow**

## I. Introduction

Models are essential to the design and operation of electric power systems. The validity of power system analyses depend on the accuracy of the model parameters. Missing or unrealistic parameters may yield inaccurate or nonsensical results.

In industry settings for which accurate results within a specific system are of the utmost importance, significant engineering efforts are devoted to identification of appropriate values in models of individual components, often drawing upon "as-built" specifications for specific elements. Conversely, research efforts often focus on characterizing the performance of computational tools across families of test systems, rather than on an outcome for a single system of interest. In such a research context, the "conventional wisdom" traditionally held that highly accurate model parameters, matched to a specific physical system, were not of great concern. (While some common test cases used by researchers [1] are based on real power systems, these test cases are generally not intended to model presently existing system facilities. Indeed, economic and security concerns often prohibit release of confidential power system models.) However, as the computational power of research tools has expanded to allow studies of large-scale test cases, this conventional wisdom has begun to shift. There has emerged growing recognition that specifics of network properties and parameter values can have significant qualitative impact on the challenge (or lack thereof) associated with a test system, and on how well these test systems reflect properties likely to be observed when applying algorithms to industry problems.

Clearly, populating test system models with parameters of at least *plausible* realism is necessary if these test systems are to be used in assessments of algorithm performance. The missing or unrealistic model parameters and constraint limits in many power system models used for research purposes introduce concerns regarding the value of numerical experiments using these models. These concerns clearly exist for dynamic models in applications such as transient stability assessment and control system design. However, this data problem becomes apparent even in the quasi-steady state context of optimal power flow (OPF) problems. In an effort to derive non-confidential, physically realistic models that are relevant to confidential optimization and power market models, previous work by some of the authors has investigated a confidentiality-preserving transformation between OPF problems [2], [3]. While such transformations may have a number of objectives, one benefit is their potential to produce test cases that may safely be publicly distributed, while preserving important qualitative properties of real-world data sets for which confidentiality must be maintained.

Complementing that work on power system model transformations, this paper addresses methods to identify and replace missing or unrealistic model parameters with the goal of improving confidence in numerical experiments conducted with publicly available data sets. This paper specifically addresses engineering-based computation of parameters for line-flow limits and generator capability curve constraints. These constraint models and parameters are used in many quasi-steady state optimization problems of current interest, including OPF studies, unit commitment problems, cascading failure simulations, and voltage stability analyses. Data sets for many existing test cases omit or provide unrealistic values for these parameters. For example, line-flow limits are missing in the commonly used data sets for the IEEE 14-, 57-, 118-, and 300-bus test systems [1].

In regard to representation of generator active and reactive power limits, the standard IEEE test systems' data sets provide information only for "box" constraints that independently limit active and reactive power generation. Further, lower limits on active power generation are set to unrealistic values of zero for the IEEE test cases. Standard textbook presentations on synchronous generator modeling confirm that the actual phys-

University of Michigan: molzahn@umich.edu, University of Wisconsin–Madison: zbfriedman@wisc.edu, lesieutre@engr.wisc.edu, demarco@engr.wisc.edu, ferris@cs.wisc.edu

ical phenomena that constrain active and reactive power output are far more accurately represented as capability curves (sometimes referred to informally as "D-curves") which capture the impacts of armature winding limits, field current limits, and end-region heating limits. Importantly in the context of market optimization, these more accurate limit models impose trade-offs between production of reactive power and active power, and therefore capture opportunity costs associated with a generator's reactive power production. The work here provides methods to identify good estimates of the more accurate capability curve limits from a data set that provides only "box-type" active and reactive limits.

The methods described in this paper are based on existing literature; indeed, much of the underlying engineering analysis is classic power systems textbook material. However, the authors hope that this paper will nonetheless provide value in reviewing and adapting these results to the needs of optimization problems of current interest. The methodology here for replacing omitted or unrealistic data is tailored to employ information that is available in typical data sets (e.g., resistances, reactances, and shunt susceptances of transmission lines, maximum active power generation capacities, rated voltage magnitudes, etc.).

This paper is organized as follows. Section II describes a method for estimating line-flow limits as multiples of the surge impedance loading values. Section III details a method for estimating generator capability curves from the box constraints on active and reactive power generation given in typical data sets. Section IV concludes the paper.

## II. Estimating Line-Flow Limits

Many power system data sets commonly used for research purposes lack realistic line-flow limits. This section estimates values for missing or unrealistic line-flow limits using two underlying quantities: the surge impedance loading (SIL) associated with the transmission line and an estimate of its length. We estimate these quantities from parameters commonly appearing in basic power flow data sets and assumptions on typically employed line geometries and material properties.

Note that analysis in this section is applicable only to transmission lines, and can not be extended to transformers. While transformers may be the limiting facilities in some operating conditions for some systems, the widely variable construction of transformers precludes general methods for estimating flow-limits from standard power flow data.

### A. Surge Impedance Loading

The surge impedance loading of a transmission line is a function of its characteristic impedance $Z_c$ and its rated voltage. A line connected to an impedance of $Z_c$ has a uniform voltage profile along the line and neither absorbs nor supplies reactive power (see, e.g., [4] for further details). The characteristic impedance is defined by the square root of the ratio of per-unit-length impedance to per-unit-length admittance; in terms of commonly available parameters:

$$Z_c = \sqrt{\frac{R + j2\pi f L}{j2\pi f C}} \tag{1}$$

where $R$ is the resistance of the line, $L$ is the inductance, $C$ is the shunt capacitance, and $f$ is the system frequency. Normalized "per unit" values for line parameters are part of typical power flow data sets, as are the base/rated voltages $V_{base}$, and system-wide power base $S_{base}$ from which the per unit normalization is defined. To obtain $Z_c$ in Ohms, convert $R$, $X$, and $C$ to Ohms, Henrys, and Farads, respectively, from per unit representation using the base impedance $Z_{base} = \frac{V_{base}^2}{S_{base}}$.

The SIL is computed from rated voltage $V_{rated}$ and characteristic impedance $Z_c$ as

$$SIL = \frac{V_{rated}^2}{|Z_c|} \tag{2}$$

SIL values for typical transmission lines are shown in Tables I and II (reproduced from Table 5.2 of [4] and Figure 7 of [5], respectively). There are several possibilities for transmission lines whose parameters yield SIL values significantly different from the values in these tables:

- The line is an underground cable, which typically have low values of $Z_c$ and correspondingly high values of SIL. The proposed method is not appropriate for underground cables, for which thermal limits are set by concerns other than conductor expansion and sag.
- The line is part of an equivalenced system. An equivalenced line does not physically exist in the system (i.e., the line parameters are chosen to match the behavior of some larger system), and thus line-flow limits cannot be estimated from a physical transmission line model.
- The electrical characteristics of other transmission facilities are combined with the line model. For instance, the impedance of a transformer at an end of the line may be combined with the line impedance, with the transformer itself not explicitly modeled.

TABLE I

Typical $Z_c$ and SIL Values (Table 5.2 in [4])

| $V_{rated}$ (kV) | $Z_c$ (Ω) | SIL (MW) |
|---|---|---|
| 69 | 366–400 | 12–13 |
| 138 | 366–405 | 47–52 |
| 230 | 365–395 | 134–145 |
| 345 | 280–366 | 325–425 |
| 500 | 233–294 | 850–1075 |
| 765 | 254–266 | 2200–2300 |

TABLE II

Typical $Z_c$ and SIL Values (Fig. 7 in [5])

| $V_{rated}$ (kV) | # Conductors | Conductor Size (kcmil) | SIL (MW) |
|---|---|---|---|
| 138 | 1 | 795 | 50.5 |
| 230 | 1 | 954 | 132 |
| 345 | 2 | 954 | 390 |
| 500 | 3 | 954 | 910 |
| 765 | 4 | 954 | 2210 |

- The transmission element represents a multi-circuit line (i.e., multiple lines on the same transmission towers). The surge impedance loading calculations in this paper do not consider the effects of multi-circuit lines.
- The line parameters are in error or are inconsistent.

For lines with shunt susceptance set to zero (i.e., the "short line" model), one cannot determine the value of SIL directly from the line parameter data. Instead one should employ the representative SIL values appropriate to the line's voltage level, as given in Tables I and II.

### *B. Line Length*

After determining the SIL, one needs to estimate the line length. Typical data sets do not specify line lengths or convenient proxies (e.g., the latitudes and longitudes of bus locations). We therefore use some reasonable assumptions.[1]

The inductance of a line can be calculated if one knows the line length $l$, line geometry (i.e., physical spacing of the conductors) and the line material properties. With knowledge of the line reactance, we next approximate the line length using estimates of typical line geometries and material properties.

The inductance of a transmission line in Henrys is

$$L = 2 \times 10^{-7} \ln\left(\frac{D_{eq}}{D_{SL}}\right) l \qquad (3)$$

where $D_{eq}$ is the geometric mean distance (GMD) for the line conductors, which is dependent on the line geometry, and $D_{SL}$ is the geometric mean radius (GMR) for the line conductors, which is dependent on the conductor characteristics (e.g., stranding and conductor bundling). Note that quantities in (3) must be converted to SI units (meters and Henrys).

The value of $l$ can be directly calculated with knowledge of $L$, $D_{eq}$ and $D_{SL}$. We next describe how to obtain these values. Table III (reproduced from Table A.4 of [4]) provides properties for typical conductor materials. Using the conductor sizes given in Table II and the material properties from Table III, relevant GMR values for a single conductor, denoted as $D_S$, are shown in Table III.

TABLE III
CONDUCTOR MATERIAL PROPERTIES (TABLE A.4 IN [4])

| Conductor Name | Conductor Size (kcmil) | $D_S$ (feet) |
|---|---|---|
| Drake | 795 | 0.0375 |
| Cardinal | 954 | 0.0403 |

Accounting for the effects of conductor bundling, the value of $D_{SL}$ is computed from the per-conductor GMR values $D_S$. Assuming a symmetric arrangement of conductors within each bundle with a distance $d$ between conductors that is much greater than the conductor radii (i.e., $d \gg D_S$) and the number of conductors per bundle given in Table II, $D_{SL}$ is calculated as shown in Table IV. A typical distance $d$ is 18 inches [6].

The remaining quantity necessary for determination of the line length $l$ is the geometric mean distance $D_{eq}$ for the line.

[1]Note that while the methods developed in this section can be generally applied, assumptions used for the conductor properties are specific to typical transmission line construction in the United States.

TABLE IV
CALCULATIONS FOR GMR ($D_{SL}$) WITH CONDUCTOR BUNDLING [4]

| | |
|---|---|
| Two-Conductor Bundle | $\sqrt{D_S d}$ |
| Three-Conductor Bundle | $\sqrt[3]{D_S d^2}$ |
| Four-Conductor Bundle | $1.091\sqrt[4]{D_S d^3}$ |

TABLE V
INTERCONDUCTOR DISTANCE $D$ FOR VARIOUS VOLTAGES

| Voltage (kV) | Interconductor Distance $D$ (feet) | Reference |
|---|---|---|
| 115 | 3 | [7] |
| 345 | 25 | [8] |
| 500 | 40 | [8] |
| 735 | 50 | [8] |

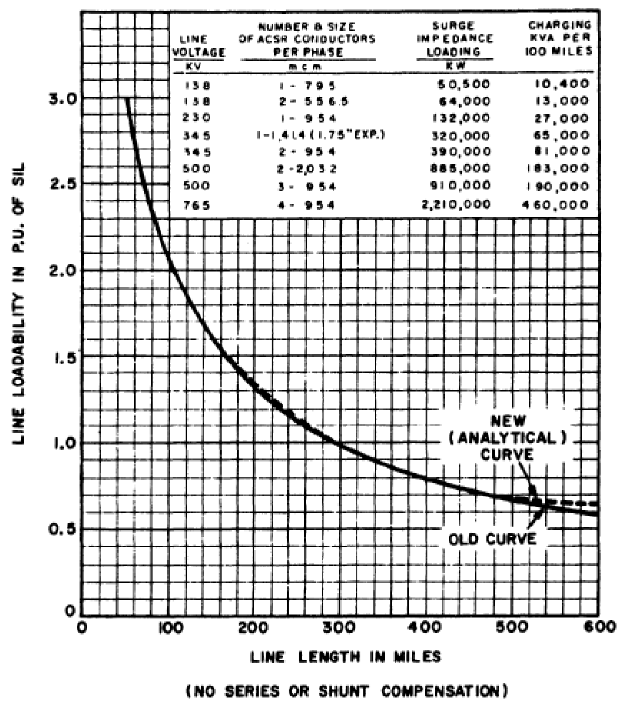


Fig. 1. Loadability Characteristic (Figure 7 of [5])

This value is a function of the interconductor distance $D$. For a completely transposed, horizontal line configuration where the interconductor distance is much greater than the bundle distance (i.e., $D \gg d$), $D_{eq}$ is calculated as

$$D_{eq} = \left(\sqrt[3]{2}\right) D \qquad (4)$$

Typical interconductor distances $D$ vary with the voltage of the transmission line; higher-voltage lines require larger interconductor distances for insulation purposes. Common values for $D$ are in Table V. To approximate the interconductor distance, we use the linear interpolation in (5) (with a minimum value of 1 foot) to estimate the interconductor distance $D$ in feet for voltages that do not appear in Table V:

$$D = 0.077\,(\text{Voltage in kV}) - 3.11 \qquad [\text{Feet}] \qquad (5)$$

With these assumptions and the inductance $L$ specified in the data set, we calculate the line length $l$ using (3). Reasonable values of $l$ range from tens to hundreds of miles.

### C. Line-Flow Limit

An estimate of the line-flow limit can now be calculated using the SIL and line length $l$. To account for short lines (less than 50 miles), enforce a maximum line-flow limit of 3.0 $\times$ SIL. For longer lines, we use the line loadability characteristic described in Fig. 1, which reproduces Figure 7 of [5].

A power function interpolation of the loadability characteristic gives the following relationship between loadability in SIL, denoted as $S^{max}$, and line length $l$.

$$\begin{aligned} S^{max} &= \text{Loadability in multiples of SIL} \\ &= 42.40\,(\text{Length in Miles})^{-0.6595} \end{aligned} \tag{6}$$

The value for $S^{max}$ should be between $0.5 \times (SIL)$ (long lines) and $3.0 \times (SIL)$ (short lines).

## III. Estimating Generator Capability Curves

Generators' capabilities are often modeled using "box" constraints for active and reactive output limits (i.e., independent limits on active and reactive power outputs). Although this model provides a starting approximation, it has the significant shortcoming that trade-offs between active and reactive power outputs are inherently neglected. A more accurate representation is that of the generator capability curve, also known as the "D-curve." This section approximates typical capability curves using machine rating standards and data from the box constraint limits typically specified in power flow data sets.

When capability curve information is available, many power flow software packages choose to employ piecewise-linear curves for its representation. The "piecewise-circular" curves defined in this section can easily be converted to piecewise-linear curves using interpolation techniques.

### A. Typical Capability Curve

The reactive power output of a synchronous generator is constrained by armature current, field current, and end-region heating limits [9]. Each of these limits, which are due to $I^2R$ heating of the corresponding section of the synchronous generator, are modeled as circles (with centers offset from the origin) in the space of active and reactive power output. The generators must operate within the intersection of these circles and within active power limits imposed by the prime mover.

We develop approximations for each of these circles using specified box constraints and typical intersection points from generator rating standards. Limits on active and reactive power generation are specified using $P^{max}$, $P^{min}$, $Q^{max}$, and $Q^{min}$.

These approximations rely on the box constraints representing a single round-rotor synchronous generator. This analysis is not applicable to box constraints that represent aggregations of generators and related equipment (e.g., capacitors, loads).

An example capability curve resulting from the method in this section is shown in Fig. 2, where $P$ and $Q$ denote the active and reactive power outputs of the generator, respectively. The upper portion of the curve is the circle from the field current limit, the right portion of the curve is the circle from the armature current limit, and the lower portion of the curve is the circle from the end-region heating limit. Each of these limits are due to $I^2R$ heating of the corresponding section of the synchronous generator.

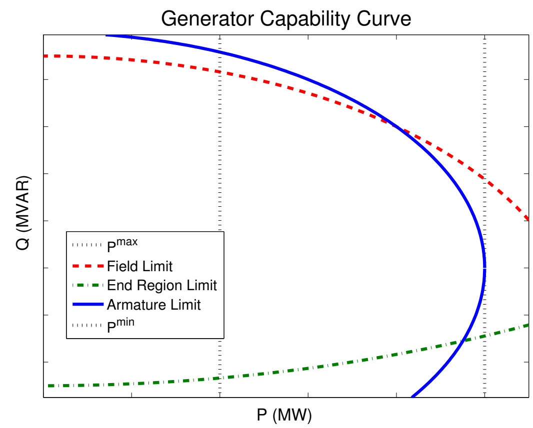


Fig. 2. Typical Generator Capability Curve

### B. Armature Current Limit

The armature current limit is described by a circle with center at the origin:

$$P^2 + Q^2 \leq (S^{max})^2 \tag{7}$$

where $S^{max} = \max(P^{max}, Q^{max})$ is the rated MVA of the generator.

A value of $S^{max}$ that is less than $P^{max}$ is interpreted as a maximum mechanical input power limit that is below the maximum electrical power generation limit of the synchronous generator. For such cases, a maximum active power limit of $P^{max}$ must also be imposed on the capability curve.

### C. Field Current Limit

Lacking data associated with detailed generator models [9], this section proposes a method by which standard machine ratings may be used to approximate the field current limit. Recognizing that the feasible set for the field current limit is a simple circle in the P-Q plane, its specification requires just the center point $\left(P_0^{field}, Q_0^{field}\right)$ and the radius $\left(r^{field}\right)$.

We first use the fact that the field current limit is centered on the $Q$-axis; that is, $P_0^{field} = 0$ [9]. We then assume that the maximum reactive power output $Q^{max}$ is achieved at zero active power output, which yields the point $(0, Q^{max})$. Finally, we use the fact that standard machine specifications use rated power factor as the intersection between the field current limit and the armature current limit. Assuming a rated power factor of 0.80 lagging, this gives a second point on the circle: $(0.8S^{max},\, 0.6S^{max})$. Corresponding parameters are

$$Q_0^{field} = \frac{(Q^{max})^2 - (S^{max})^2}{2\,(Q^{max} - 0.6S^{max})} \tag{8a}$$

$$r^{field} = Q^{max} - Q_0^{field} \tag{8b}$$

The resulting field current limit is

$$P^2 + \left(Q - Q_0^{field}\right)^2 \leq \left(r^{field}\right)^2 \tag{9}$$

The relative values of $Q^{max}$ and $P^{max}$ result in three cases:

1) If $Q^{max} \geq P^{max}$, then $S^{max} = Q^{max}$ and $Q_0^{field} = 0$, resulting in the same armature and field current limits.
2) If $Q^{max} \leq 0.6P^{max}$, then $Q_0^{field}$ is non-negative. Only negative values of $Q_0^{field}$ are physically meaningful [9]. Accordingly, if $Q_0^{field} \geq 0$, we impose a fixed upper limit (i.e., $Q \leq Q^{max}$) and disregard the value of $Q_0^{field}$.
3) If $P^{max} > Q^{max} > 0.6P^{max}$, which is expected to be the case for typical generators, the armature and field current limits impose distinct constraints.

### *D. End-Region Heating Limit*

Limits on leading power factor operation of a synchronous generator are due to end-region heating. To approximate the end-region heating limit, we assume 1) the end-region heating limit takes the form a circle with center $\left(P_0^{end}, Q_0^{end}\right)$ on the $Q$-axis (i.e., $P_0^{end} = 0$) and radius $r^{end}$, 2) the point $\left(0, Q^{min}\right)$ is on this circle, and 3) the intersection of this limit with the armature current limit occurs at 0.95 leading power factor as in [10]. These assumption lead to

$$P^2 + \left(Q - Q_0^{end}\right)^2 \leq \left(r^{end}\right)^2 \tag{10a}$$

$$Q_0^{end} = \frac{\left(Q^{min}\right)^2 - (S^{max})^2}{2\,(Q^{min} + 0.31S^{max})} \tag{10b}$$

$$r^{end} = Q_0^{end} - Q^{min} \tag{10c}$$

The relative values of $Q^{min}$ and $S^{max}$ result in three cases:

1) If $\left|Q^{min}\right| \leq 0.31S^{max}$, then $Q_0^{end}$ is non-positive. Only positive values of $Q_0^{end}$ are physically meaningful [9]. Accordingly, if $Q_0^{end} \leq 0$, we impose a fixed lower limit (i.e., $Q \geq Q^{min}$) and disregard the value of $Q_0^{end}$.
2) If $S^{max} \geq \left|Q^{min}\right| > 0.31S^{max}$, which is expected to be the case for typical generators, the armature and field current limits impose distinct circle constraints.
3) The case $\left|Q^{min}\right| > S^{max}$ is atypical for synchronous generators. For this case, the armature current limit is binding before the specified $Q^{min}$; that is, the synchronous generator cannot actually reach $Q^{min}$ due to the armature current limit. If this case does occur, use the specified lower limit (i.e, $Q \geq Q^{min}$) and ignore the armature current limit for negative values of $Q$. In other words, use the original box constraints for the lower half of the generator capability curve.

### *E. Prime Mover Limits*

Limits on the mechanical input power from the prime mover impose simple upper and lower bounds on achievable active power generation. The maximum and minimum active power generation $P^{max}$ and $P^{min}$ are given by the box constraints.

For thermal generators, realistic minimum active power generation levels are typically significantly greater than zero; yet many publicly available data sets report this limit to be zero (i.e., $P^{min} = 0$), suggesting missing or incorrect data. Reference [11] describes a statistical study of the minimum economic operating point ("eco-min") for thermal generators. To estimate $P^{min}$, this section uses the results from [11] that correspond to information in many public data sets.

Typical data sets specify generators' nameplate capacity (i.e., $P^{max}$) and may provide generators' prime mover type. If both of these data fields are available, we use the median eco-min data specified in Figs. 15, 23, and 25 of [11] to approximate $P^{min}$. The data from these figures is reproduced in Table VI, which considers steam turbines and combined-cycle prime movers, and Table VII, which considers combustion-turbine prime movers operated both independently and as part of a combined-cycle plant. Note that [11] suggests that there may be substantial variance around these median data.

If the data set does not include the prime mover type, we use the averages among all prime mover types from Table VIII, which is reproduced from Fig. 10 of [11], to specify $P^{min}$ based on the nameplate capacity data only.

TABLE VI
TYPICAL $P^{min}$ FOR STEAM TURBINES AND COMBINED-CYCLE PRIME MOVERS (FIGS. 15 AND 23 IN [11])

| $P^{max}$ | Steam Turbine | Combined Cycle |
|---|---|---|
| 0-200 MW | 38% | 80% |
| 200-400 MW | 39% | 46% |
| 400-600 MW | 49% | 41% |
| 600-800 MW | 60% | 48% |
| $>$ 800 MW | 64% | 42% |

TABLE VII
TYPICAL $P^{min}$ FOR COMBUSTION-TURBINE PRIME MOVERS (FIG. 25 IN [11])

| $P^{max}$ | Independently Operated CT | CT in Combined Cycle Plant |
|---|---|---|
| 0-50 MW | 76% | 80% |
| 50-100 MW | 66% | 95% |
| 100-150 MW | 59% | 63% |
| 150-200 MW | 81% | 63% |
| 200-250 MW | 71% | 58% |
| 250-300 MW | – | 64% |

TABLE VIII
TYPICAL $P^{min}$ WITHOUT PRIME MOVER DATA (FIG. 10 IN [11])

| $P^{max}$ | $P^{min}$ |
|---|---|
| 0-200 MW | 69% |
| 200-400 MW | 42% |
| 400-600 MW | 45% |
| 600-800 MW | 48% |
| $>$ 800 MW | 69% |

## IV. Conclusion

It is obvious that use of power system test data sets with missing or unrealistic parameters may yield inaccurate results. Perhaps more subtly, use of these test cases may undermine research efforts seeking to characterize effectiveness of new algorithms in such problems as optimal power flow. For industry purposes, significant effort is required to accurately model the behavior of specific power system facilities and components, so that simulations based on such models provide a good match to observed physical behavior in the field. However, security and privacy concerns often preclude the dissemination of data sets closely based on real, operating physical systems to serve as publicly available test cases. Instead, research on new algorithms and analysis methods must employ test cases that are either altogether synthetic or anonymized versions of past configurations of real-world power systems. Many of these public test cases and data sets have evolved with a first objective that they provide a "reasonable" power flow solution, and often provide incomplete data and/or models to inform more advanced applications such as optimal power flow. Missing and/or unrealistic parameters in some of these test cases limits their usefulness. This paper has described methods for estimating reasonable line-flow limits and generator capability curve parameters using widely available data, supplemented by basic engineering assumptions on the nature of transmission line and synchronous generator construction. Publicly available data sets augmented with parameters estimated using the methods described in this paper are available at [12].

## References


[1] Power Systems Test Case Archive. University of Washington Department of Electrical Engineering. [Online]. Available: http://www.ee.washington.edu/research/pstca/

[2] A. Borden, D. Molzahn, B. Lesieutre, and P. Ramanathan, "Power System Structure and Confidentiality Preserving Transformation of Optimal Power Flow Problem," in *51st Annu. Allerton Conf. Commun., Control, and Comput.*, Oct. 2-4 2013.

[3] D. Wu, B. Lesieutre, and P. Ramanathan, "Feasibility of Power System Structure Preserving Linear Transformations for the AC Optimal Power Flow Problem," in *52nd Annu. Allerton Conf. Commun., Control, and Comput.*, Sept. 2014, pp. 715–722.

[4] J. Glover, M. Sarma, and T. Overbye, *Power System Analysis and Design*. Thompson Learning, 2008.

[5] R. Gutman, P. Marchenko, and R. Dunlop, "Analytical Development of Loadability Characteristics for EHV and UHV Transmission Lines," *IEEE Trans. Power App. and Syst.*, vol. PAS-98, no. 2, pp. 606–617, Mar. 1979.

[6] F. Kiessling, P. Nefzger, J. F. Nolasco, and U. Kaintzyk, *Overhead Power Lines: Planning, Design, Construction*. Springer, 2003.

[7] L. Barthold, R. Clayton, I. Grant, V. Longo, J. Stewart, and D. Wilson, "Transmission Line Reference Book: 115–138 kV Compact Line Design," Electric Power Research Institute, Inc., Palo Alto, CA, Tech. Rep., 1978.

[8] D. MacCarthy, "EHV Transmission Line Reference Book," *Project EHV, General Electric Company, Edison Electric Institute*, 1968.

[9] P. Kundur, N. Balu, and M. Lauby, *Power System Stability and Control*. McGraw-hill New York, 1994.

[10] J. Jackson, "Interpretation and Use of Generator Reactive Capability Diagrams," *IEEE Trans. Ind. Appl.*, no. 6, pp. 729–732, 1971.

[11] "Eco-Min Estimation," Federal Energy Regulatory Commission Staff Report, Tech. Rep., draft version. Final version to appear at http://www.ferc.gov/industries/electric/indus-act/market-planning/opf-papers.asp.

[12] Power Systems Case Study. University of Wisconsin–Madison. [Online]. Available: http://neos-dev-web.neos-server.org/guide/?q=power